Araştırma Makalesi / Research Article

Gamma-ray Shielding Properties of Lithium Borate Glass Doped with Colemanit Mineral

Nergiz YILDIZ YORGUN*

Van Yüzüncü Yıl University, Deparment of Physics, Van
(ORCID: 0000-0002-2515-1994)

Abstract
In this study, $(Li2B4O7)_{(100-x)}$-$(Colemanite)_x$ glass systems (where x=10, 20, 30 and 40 wt %) were fabricated via melt quenching technique. The radiation shielding parameters of produced glasses such as mass attenuation coefficient (μ_m), effective atomic number (Z_{eff}), electron density (N_{el}), half value layer (HVL) and mean free path (MFP) were measured experimentally for 81, 276, 302, 356, and 383 keV gamma ray energies with Hp-Ge detector. Also, WinXCom software was employed for theoretical calculation above radiation shielding parameters of glasses for 1 keV to 10^5 MeV energy region. It was seen that the experimental and theoretical results are good agreement with each other. The obtained results revealed that when percentage of colemanite mineral has been increased in the glass system, μ_m, Z_{eff} and N_{el} values increase. Furthermore, it was observed that the values of HVL and MFP, in contrary, decreases with increasing colemanite mineral percent. In specific, among the investigated glasses, lithium borate glass with 40 percentage colemanite mineral has the highest value of μ_m, Z_{eff} and N_{el}, however, it has the lowest HVL and MFP. Therefore, lithium borate glass with 40 percentage colemanite mineral has given the best results for gamma radiation shielding purpose among the investigated glass systems in this work.

Keywords: Colemanit, lithium borate, mass attenuation coefficient, effective atomic number, half value layer, mean free path

Kolemanit Minerali ile Katkılanmış Lityum Borat Camların Gama-ışını Zırh Özellikleri

Öz
Bu çalışmada, $(Li2B4O7)_{(100-x)}$ - $(Kolemanit)_x$ cam sistemler (burada x = 10, 20, 30 ve % 40 ağırlık) erime söndürme tekniği ile üretildi. Üretilen camların, kütle soğurma katsayısı (μ_m), etkin atom numarası (Z_{eff}), elektron yoğunluğu (N_{el}), yarı değer kalınlıkları (HVL) ve ortalama serbest yol (MFP) gibi radyasyon zırh parametreleri 81, 276, 302, 356 ve 383 keV gama enerjilerinde deneysel olarak Hp-Ge dedektörü ile ölçüldü. Ayrıca, camların bu radyasyon zırh parametrelerinin 1 keV-10^5 MeV enerji aralığında teorik hesaplamaları için WinXCom programı kullanıldı. Deneysel ve teorik sonuçların birbirleri ile iyi uyum içinde olduğu görüldü. Elde edilen sonuçlar, cam sistemindeki kolemanit mineralinin yüzdesi arttığında, μ_m, Z_{eff} ve N_{el} değerlerinin de arttığını ortaya koydu. Ayrıca, bunun aksine, kolemanit yüzdesinin artmasıyla HVL and MFP değerlerinin azaldığı gözlendi. Spesifik olarak, incelenen camlar arasında yüzde 40 kolemanit mineral içeriğine sahip lityum borat cam en yüksek μ_m, Z_{eff} ve N_{el} değerine sahip, bununla birlikte en düşük HVL ve MFP'ye sahiptir. Bu nedenle, bu çalışmada, incelenen cam sistemleri arasında %40 kolemanit minerali içeren lityum borat cam gama radyasyonu zırh özellikleri için en iyi sonucu vermiştir.

Anahtar Kelimeler: Kolemanit, lityum borat, kütle soğurma katsayısı, etkin atom numarası, yarı değer kalınlığı, ortalama serbest yol

*Sorumlu yazar: nergiz_yildizr@yahoo.com
Geliş Tarihi: 11.02.2019, Kabul Tarihi: 01.07.2019

1. Introduction

X-rays and gamma rays emitted by radiation sources, which are used in medical treatment, nuclear power plants, agriculture, engineering, radiation biophysics, space technology, nuclear diagnostics etc…, are dangerous to human health and precision laboratory instruments [1]. For instance, direct exposure to gamma radiation with ionizing property can cause organ failure, cancer, skin rash, and genetic damage. Even if human being are exposured to high dose gamma radiation, the result could be death [2]. To minimize harmful effects of gamma and X-rays on human health and instruments, shielding materials have been used. The ideal materials for gamma rays shielding should have some desirable properties such as elements with high atomic number, economically cheap, abundant materials on earth, flexible for applying to any design etc…[3]. Many studies on gamma radiation shielding have been performed by researchers, using different materials such as concrete [4,-7], alloy [8-10] polymer [11,12]. During the last few years, many researchers have paid attention on glass type shielding materials due to transparent property, easy shaped, easy transportation and having properties for attenuation of neutron and photons [13]. Nowadays, many researches related with different type of glass such as Pb-Based Silicate, Borate, and Phosphate glasses [14] heavy metal oxide glasses [15,16], heavy metal fluoride based tellurite-rich glasses [17], optical glasses [18], bismuth borate glasses [19] have been carried out to determine shielding properties. Lithium borate glasses (LBGs) could be good candidate for shielding purpose among the other type of glasses due to high radiation resistance, linear dose dependence in a wide range of doses and high transparency in the spectral range from vacuum ultraviolet to the far infrared region [20].

Colemanite ($2CaO.3B_2O_3.5H_2O$) is calcium borate mineral. It is one of the fairly used aggregate added in radiation shielding concrete because of its the least soluble property as a natural borates [21].

After very intense literature search, I could not come cross any theoretical or experimental studies related with investigation of radiation shielding properties of lithium borate glasses doped with colemanite mineral. Therefore, this study will be guide to researchers who performs on the LBGs systems.

The main parameters of gamma shielding interaction with materials are counted as a mass attenuation coefficient, effective atomic number, half-value layer, and mean free. In this study, these parameters for lithium borate glasses doped without and with colemanite mineral in various percentage were determined not only with experimental method, but also with WinXCom software in the energy range 1keV-100GeV.

2. Material and Method

2.1. Theoretical Calculations

2.1.1. Mass attenuation coefficient

If monochromatic-ray pass through matter, a part of them is absorbed. The decrease in radiation intensity is expressed by an exponential equation containing parameters related to the given case [22]:

$$I = I_0\, e^{-\mu x} \tag{1}$$

where I is the intensity of transmitting radiation; I_0 is the incident radiation intensity; μ represents the linear attenuation coefficient, cm^{-1}; x stand for the material thickness, cm.

The mass attenuation coefficient, $\mu_m = \frac{\mu}{\rho}$, is related to unit density (ρ, g/cm^3); then Equation 1 have the following form:

$$I = I_0\, e^{\mu_m \rho x} \tag{2}$$

If target consist of mixture and compound, the mass attenuation coefficient is calculated via WinXCom software according to mixture law [23].

$$\mu_m = \sum_i P_i \ \mu_{m,i} \quad (3)$$

where P_i and $\mu_{m,i}$ are the weight fraction and mass attenuation coefficient, respectively, of the constituent element i [th].

$$\sum_i P_i = 1 \quad (4)$$

2.1.2. Effective atomic number and electron density

Effective atomic number, Z_{eff}, represents interaction between gamma-ray and absorbent composed from various elements Effective atomic number is written in the form following [24] :

$$Z_{eff} = \frac{\sum_i f_i A_i \mu_{m,i}}{\sum_j f_j \frac{A_j}{Z_j} \mu_{m,j}} \quad (5)$$

where f_i is the fraction by mole of each constituent element, providing that $\sum_i f_i = 1$, A_i is the atomic weight, Z_j is the atomic number and $\mu_{m,i}$ is the mass attenuation coefficient of i[th] element.
Effective electron density, N_{el}(electrons/gram), describes the number of electrons per unit mass of the interacting materials and it is given with following formula [25].

$$N_{el} = N_A \frac{nZ_{eff}}{\sum_i n_i A_i} = N_A \frac{Z_{eff}}{A} \quad (6)$$

here, A is the mean atomic mass and N_A is Avogadro constant.

2.1.3. Half value layer and mean free path

Half value layer (HVL) is the thickness of a given material which decreases the intensity of radiation to half of its original value as a follows [26]:

$$HVL = \frac{0.693}{\mu} \quad (7)$$

Mean free path (MFP) is the average distance which a photons travels in medium before an interactions occurs (or between successive interactions) and have been calculated using the following relation [27]:

$$MFP = \frac{1}{\mu} \quad (8)$$

3. Experimetal Method

3.1. Preparation of sample

Doping mineral colemanite is mined at Kutahya province in Turkey (Emet, Hisarcık areas) and its chemical content was determined by X-ray diffraction(XRF) [28]. Then, to fabricate pure LBG, the rapid melt quenching technique was employed. In this technique, lithium borate powder was melted within a platinum crucible of an electrical furnace at the temperature of 1000°C for 30 min. Obtained melt was poured in a disc-shaped platinum plate. After that, desired percentage colemanite element was added to lithium borate powder and above procedure was repeated to fabricate aimed glass samples. The prepared samples have 37mm diameter and their thicknesses are 3.6 $\pm$0.02 mm. The pure lithium borate glass was used as a reference sample and labeled with R. According to added percentage of colemanite mineral, samples were labeled with C1, C2, C3 and C4 for 10%, 20%, 30% and 40%, respectively. Density of glass samples was measured via Archimede's principle (Table1).

3.2. Gamma-ray transmission measurements

In this study, HpGe detector was used to measure photon interaction parameters of lithium borate glass with and without doping minerals. Gamma photons, which are emitted from 3Ci ^{133}Ba point source, with 81,276,302,356 and 383 keV energies were used to irradiate samples. After irradation progress, the photo peak density was measured before and after sample was placed between radioactive source and detector (Figure 1). The spectrums were recorded using the computer software MAESTRO (6.08 version) with a multichannel analyzer. The data for every measurements were collected for one hour and the measurement for each sample were repeated 3 times. The mass attenuation coefficient value was calculated after value of I_0 and I were inserted in Equ-1.
The experimental uncertainty of attenuation coefficient measurements for the fabricated glasses has been estimated by relation [29]:

$$\Delta\left(\frac{\mu}{\rho}\right) = \frac{1}{\rho x}\sqrt{\left[\left(\frac{\Delta I_0}{I_0}\right)^2 + \left(\frac{\Delta I}{I}\right)^2 + ln\left(\frac{\Delta I}{I}\right)^2 . \left(\frac{\Delta \rho x}{\rho x}\right)^2\right]}$$

where $\Delta\rho x$ denotes the uncertainty in the mass per unit area, ΔI_0 and ΔI are the uncertainty in the intensities I_0, I , respectively.

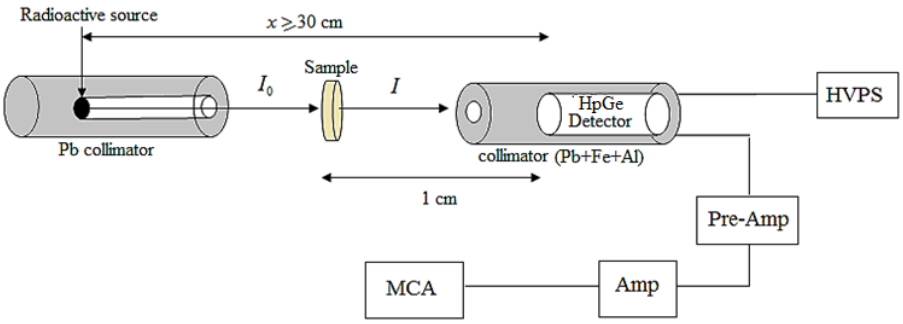

Figure 1. Experimental set up for measurement

4. Result and Discussion

The mass attenuation coefficients (μ_m) values obtained from experimental measurement with 3 % statistical error and theoretical calculation were inserted in Table 1. As seen from Table 1, theoretical and experimental findings are good agreement each other in experimental energy limits. Moreover, while values of μ_m decrease with increasing photon energies, it increases with increasing colemanite mineral percentage. Figure 2a demonstrates theoretical μ_m values calculated by WinXCom software versus incident photon energy for 1 keV to 10^5 MeV. In Figure 2a, energy scale could be divided in three energy zone according to dominate γ-photons interaction: photoelectric effect (E< 0.05 MeV), Compton scattering (0.05 MeV< E < 30 MeV) and pair production (E > 30 MeV). In photoelectric zone (Figure 2b), value of μ_m decrease sharply with increasing energy for investigated LBG's. This case could be explained that microscopic cross section is inversely correlated with incoming photon energy $E^{-3.5}$, however, it is directly proportional to LBGs atomic number, Z^{4-5} for photoelectric effect. Figure 2c shows how values of μ_m change with energy in Compton zone. The values of μ_m slowly decrease and the difference of μ_m values of LBGs is almost zero. The reason behind the variation in μ_m with energy depends on cross section of compton scattering which is related linearly to atomic number (Z). After 30 MeV corresponding to pair production region (Figure 2d), μ_m slightly increase and then stay almost constant (for γ-ray energies $>10^3$ MeV). This case is explained with Z^2 dependence of pair production process [30]. The highest value of μ_m belongs to C4 sample, on the contrary, R sample has the lowest value.

Table 1. μ_ρ , Z_{eff} and HVL values of glasses acquired as theoretically and experimentally

	$Li_2B_4O_7$ (Ref. Glass) 2.210±0.004 g/cm³		Colemanite %10 2.254±0.004 g/cm³		Colemanite %20 2.271±0.004 g/cm³		Colemanite %30 2.288±0.004 g/cm³		Colemanite %40 2.306±0.004 g/cm³	
Energy	μ/ρ (cm²/g)									
(MeV)	Theo.	Expt.	Theo.	Expt.	Theo.	Expt.	Theo.	Expt.	Theo.	Expt.
0.081	0.1593	0.1590± 0.0047	0.1631	0.1598±0.0041	0.1661	0.162±0.0042	0.1690	0.1684±0.0054	0.1720	0.1752±0.0051
0.276	0.1068	0.1065±0.0031	0.1070	0.1112±0.0035	0.1082	0.110±0.0035	0.1091	0.1121±0.0033	0.1092	0.1108±0.0034
0.302	0.1032	0.1030±0.0030	0.1042	0.0995±0.0024	0.1041	0.106±0.0034	0.1055	0.1092±0.0037	0.1057	0.1084±0.0032
0.356	0.0971	0.0973±0.0029	0.0987	0.0957±0.0022	0.0981	0.101±0.0032	0.0994	0.1128±0.0035	0.0999	0.1032±0.0032
0.383	0.0942	0.0940±0.0028	0.0953	0.0924±0.0027	0.0949	0.098±0.0024	0.0961	0.1005±0.0034	0.0966	0.0965±0.0024
Energy	$Z_{eff.}$ (electron/atoms)									
(MeV)	Theo.	Expt.	Theo.	Expt.	Theo.	Expt.	Theo.	Expt.	Theo.	Expt.
0.081	6.7591	6.7480±0.2024	6.9881	6.8178±0.2041	7.1867	7.0134±0.2104	7.3854	7.342±0.2202	7.7849	7.9205±0.2370
0.276	6.7478	6.7287±0.2018	6.9413	7.2012±0.2162	7.1906	7.3232±0.2199	7.4411	7.646±0.2291	7.8890	7.9472±0.2387
0.302	6.7538	6.7378±0.2021	6.9869	6.6506±0.1995	7.1704	7.3087±0.2195	7.4247	7.707±0.2312	7.8885	8.0834±0.2426
0.356	6.7534	6.7695±0.2030	7.0034	6.7899±0.2033	7.1892	7.4095±0.2227	7.4506	8.428±0.2524	7.8902	8.2060±0.2469
0.383	6.7541	6.7364±0.2020	6.9938	6.7735±0.2032	7.1797	7.4067±0.2228	7.4434	7.753±0.2327	7.8897	7.9555±0.2387
Energy	HVL(cm)									
(MeV)	Theo.	Expt.	Theo.	Expt.	Theo.	Expt.	Theo.	Expt.	Theo.	Expt.
0.081	1.9687	1.9725±0.0594	1.8852	1.9340±0.1301	1.8372	1.8842±0.127	1.7925	1.8032±0.1234	1.7470	1.7174±0.1182
0.276	2.9364	2.9447±0.0882	2.8743	2.7702±0.1875	2.8205	2.7745±0.189	2.7764	2.7045±0.1856	2.7521	2.7325±0.1894
0.302	3.0394	3.0447±0.0915	2.9514	3.1065±0.2104	2.9117	2.8790±0.196	2.8719	2.7795±0.1901	2.8600	2.7832±0.1925
0.356	3.2307	3.2235±0.0971	3.1385	3.2368±0.2182	3.1118	3.0212±0.205	3.0474	2.7043±0.1856	3.0368	2.9185±0.2017
0.383	3.3301	3.3364±0.1001	3.2368	3.3425±0.2251	3.2157	3.1144±0.212	3.1529	3.0296±0.2074	3.1272	3.1309±0.2145
Energy	N_{el}x10^{23} (electron/gram)									
(MeV)	Theo.	Expt.	Theo.	Expt.	Theo.	Expt.	Theo.	Expt.	Theo.	Expt.
0.081	2.9214	2.9178±0.0875	2.9392	2.8673±0.0864	2.9434	2.8721±0.0862	2.9481	2.931±0.087	2.9203	2.9715±0.0892
0.276	2.9170	2.9081±0.0873	2.9197	3.0285±0.0906	2.9447	2.9993±0.0895	2.9704	3.052±0.091	2.9598	2.9817±0.0894
0.302	2.9191	2.9126±0.0872	2.9384	2.7978±0.0832	2.9367	2.9931±0.0893	2.9649	3.077±0.092	2.9595	3.0325±0.0901
0.356	2.9198	2.9265±0.0875	2.9454	2.8555±0.0851	2.9442	3.0349±0.0917	2.9747	3.364±0.100	2.9597	3.0788±0.0928
0.383	2.9193	2.9127±0.0874	2.9416	2.8482±0.0851	2.9406	3.0332±0.0904	2.9716	3.095±0.092	2.9599	2.9845±0.0898
Energy	MFP(cm)									
(MeV)	Theo.	Expt.	Theo.	Expt.	Theo.	Expt.	Theo.	Expt.	Theo.	Expt.
0.081	2.8409	2.8460±0.0856	2.7203	2.7901±0.0845	2.6511	2.7185±0.0783	2.5866	2.6025±0.074	2.5214	2.4780±0.0742
0.276	4.2372	4.2498±0.1272	4.1476	3.9979±0.1205	4.0700	4.0032±0.1207	4.0112	3.9025±0.116	3.9714	3.9425±0.1189
0.302	4.3859	4.3937±0.1325	4.2558	4.4812±0.1346	4.2301	4.1545±0.1256	4.1442	4.0102±0.129	4.1034	4.0152±0.1209
0.356	4.6620	4.6507±0.1403	4.4964	4.6704±0.1409	4.4903	4.3607±0.1312	4.3975	3.9027±0.113	4.3426	4.2105±0.1264
0.383	4.8053	4.814±0.1443	4.6554	4.8221±0.1459	4.6403	4.4938±0.1359	4.5495	4.3717±0.132	4.4903	4.5170±0.1367

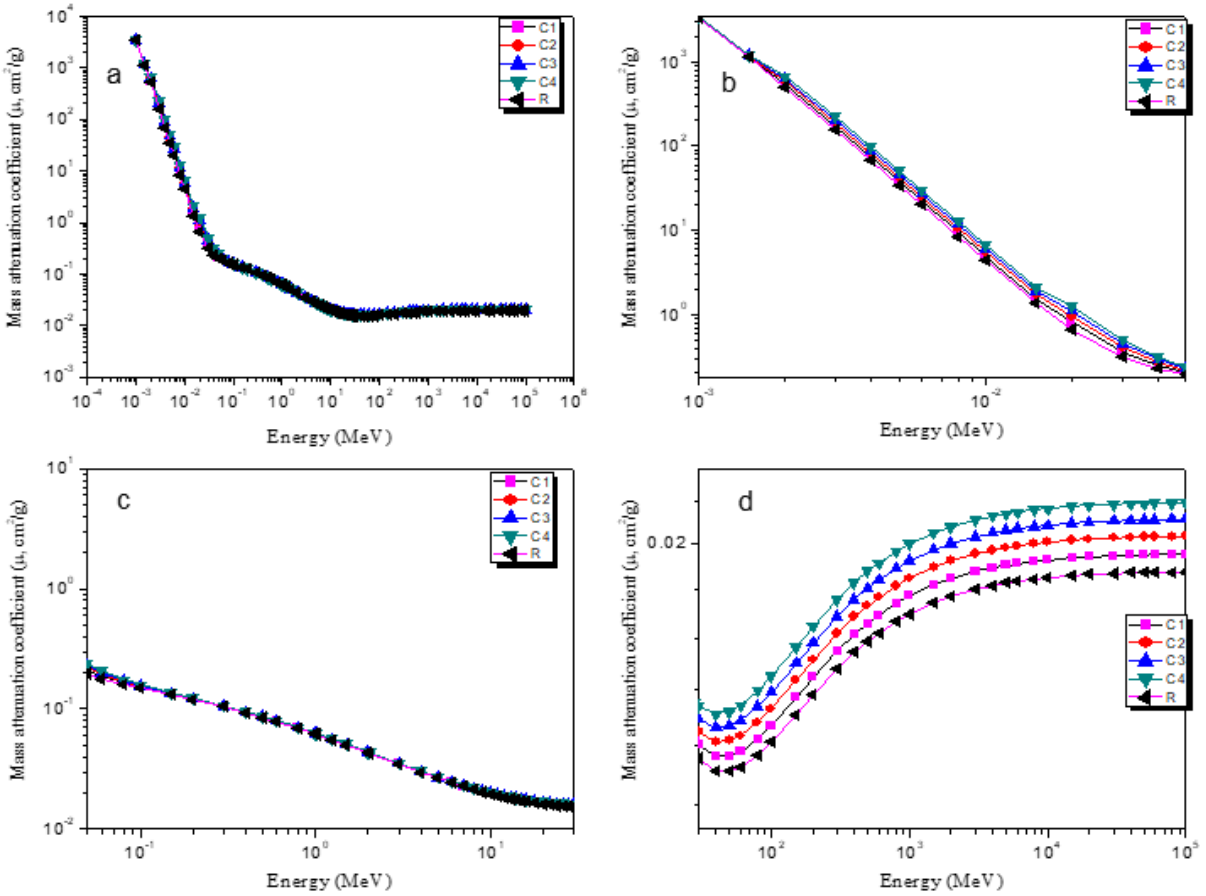

Figure 2. Mass attenuation coefficients for the selected glasses in (a) the total energy region (1KeV<E<10^5 MeV) and (b) the low energy region E>0.05 MeV (c) the energy region 0.05 MeV< E < 30 MeV (d) the energy region E > 30 MeV

The Table 1, demonstrate Z_{eff} ve N_{el} values measured and calculated at selected energy values. As seen from tables, they are in good harmony with each other. Also, Figure 3 - 4 present Z_{eff} ve N_{el} for incident photon energy (1keV$\leq E \leq 10^5$ MeV). R, C1, C2, C3 and C4 samples have same characteristic behavior for Z_{eff} (Figure3). In low energy region (1keV - 0.015 MeV), Z_{eff} and N_{el} have the highest values (Figure 3-4) for with and without doping minerals of LBG. In specific, the value of Z_{eff} ve N_{el} sharply decrease with incident γ-ray in the range of 0.015 MeV and 0.02 MeV due to photoelectric effect . After 0.02 MeV, they start rise till 0.3 MeV and stay constant for rest of incident gamma-ray energy. Moreover, the value of Z_{eff} increases with increasing percentage of colemanite in system. Same behavior is also observed for N_{el} due to close relation with Z_{eff}. These result also supports to Hine findings [31].

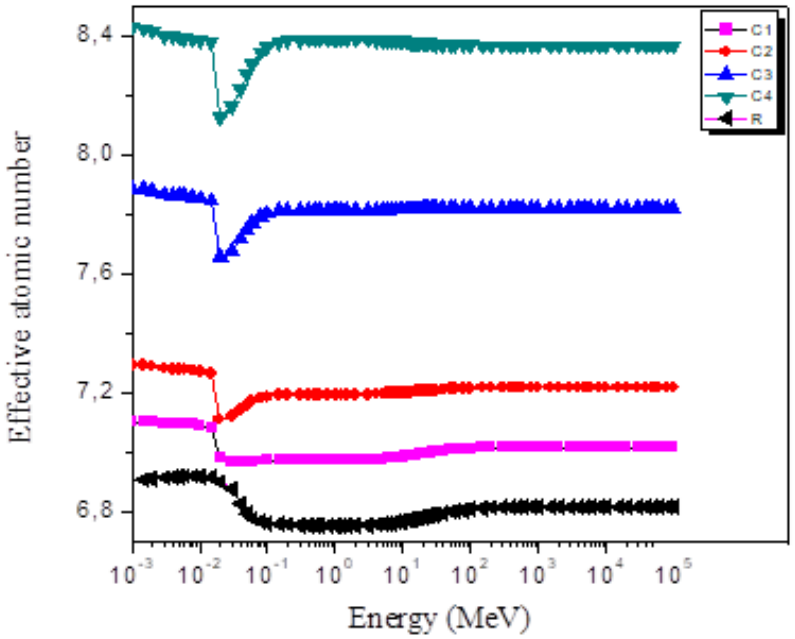

Figure 3. Variation of effective atomic numbers against photon energy of lithium borate glasses

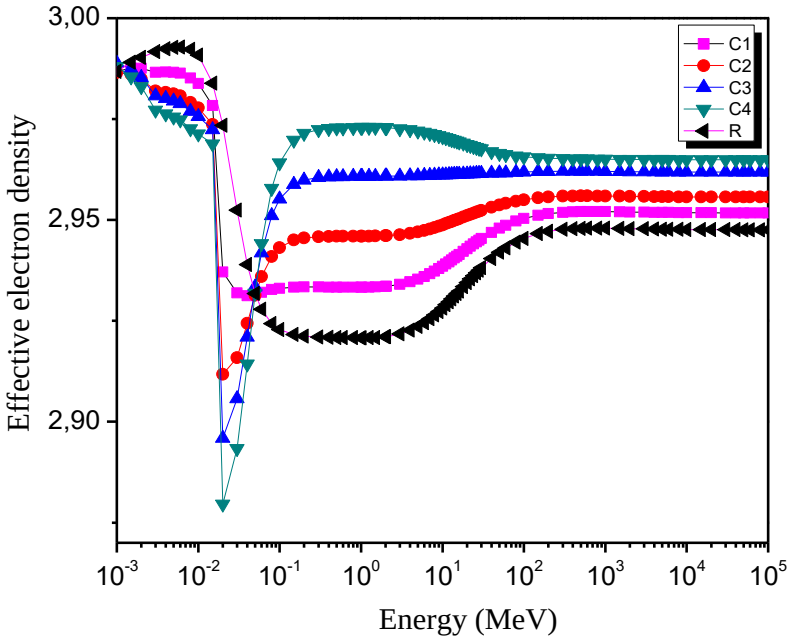

Figure 4. Variation of electron density against photon energy of lithium borate glasses

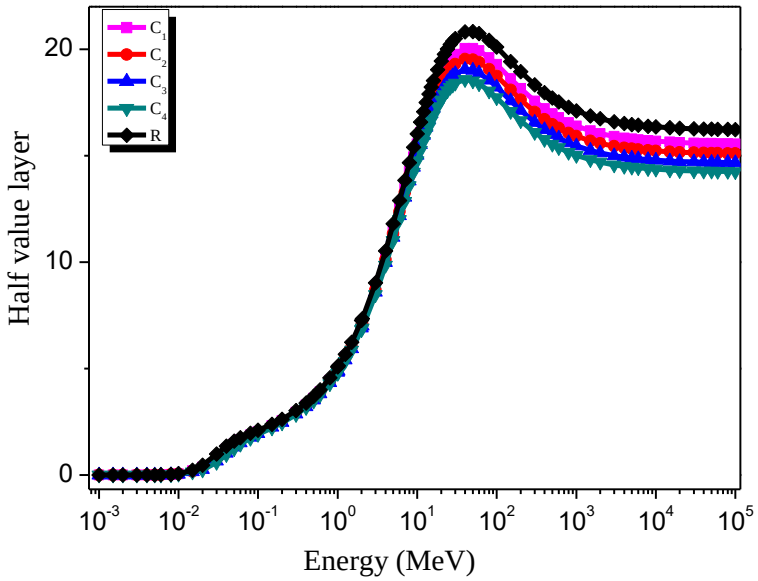

Figure 5. Half value layer (HVL) against photon energy of lithium borate glasses

Half value thicknesses (HVL) and mean free path (MFP) of all samples are also calculated and inserted in Table 1 for the same energy values. In experimental set up limit, the obtained values of HVL and MFP from theoretical calculation agree fairly well with experimental results. Also, Figures 5 and 6 represents HVL and MFP versus incident gamma energies, respectively. As seen from Figure 5 and 6, HVL and MFP have the lowest value and independent from colemanite percentage and incident gamma ray energy in the low energy region ($< 0.01\ MeV$). In intermediate region ($0.01\ \text{MeV} < E < 30\ MeV$), the values of HVL and MFP rise sharply. Moving further the high energy region, the HVL and MFP values gets smoother and it stays constant after 2000 MeV. One more detail, while the highest values of HVL and MFP belong to R sample, C4 sample has the lowest values for both parameters which indicates that C4 sample has high shielding capacity.

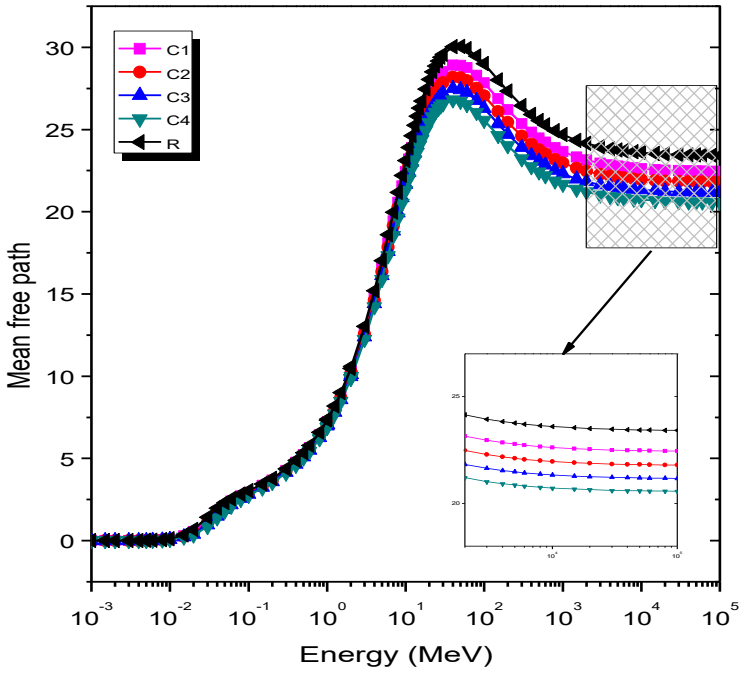

Figure 6. Mean free path (mfp) against photon energy of lithium borate glasses

5. Conclusion

In present work, pure and various percentage colemanite doped lithium borate glasses were fabricated. Using both experimental and theoretical methods, photon interaction parameters such as mass attenuation coefficient (μ_m), effective atomic number (Z_{eff}),electron density (N_{el}), half value layer (HVL) and mean free path (MFP) of LBGs were measured and calculated, respectively. It was observed that the obtained theoretical and measured experimental results verify each other in the experimental energy region limit. Increasing percentage of colemanite mineral in glass systems results to higher mass attenuation coefficient value. On the contrary, the value of mass attenuation coefficient decreases with increasing energy. The μ_m gets higher value in the low energy region where photoelectric phenomena dominates and it has smaller value in the middle energy region where Compton scattering is main process. Among the fabricated glass system, LBG doped with 40 % colemanite mineral has the highest μ_m value. The parameters Z_{eff} and N_{el} are strictly related to photon energy and the percentage rate of colemanite mineral in LBGs systems. The higher values of both parameters are in the lower energy region where the photoelectric effect dominates. To gain better shielding properties, material should have the lower HVL and MFP value which indicates more interaction between gamma rays and material. According to obtained results, LBG doped with colemanite mineral 40 %, which is transparent, could be considered as a shielding material against γ- radiation used in various technological areas.

References

[1] Chanthima N., Kaewkhao J. 2013. Investigation on radiation shielding parameters of bismuth borosilicate glass from 1 keV to 100 GeV. Annals of Nuclear energy, 55: 23-28.

[2] Kaur P., Singh K.J., Thakur S., Singh, P., Bajwa B.S. 2019 Investigation of bismuth borate glass system modified with barium for structural and gamma-ray shielding properties. Spectrochimica Acta Part A: Molecular and Biomolecular Spectroscopy, 206: 367-377.

[3] Singh V.P., Badiger N.M., Chanthima N., Kaewkhao J. 2014. Evaluation of gamma-ray exposure buildup factors and neutron shielding for bismuth borosilicate glasses. Radiation Physics and Chemistry, 98: 14-21.

[4] Akkurt I., Basyigit C., Kilincarslan S., Mavi, B., Akkurt, A. 2006. Radiation shielding of concretes containing different aggregates. Cement and Concrete Composites, 28: 153-157.

[5] Akkurt I., Akyıldırım H., Mavi B., Kilincarslan S., Basyigit, C. 2010. Radiation shielding of concrete containing zeolite. Radiation Measurements, 45: 827-830.

[6] Kharita M.H., Yousef S., Al Nassar M. 2011. Review on the addition of boron compounds to radiation shielding concrete. Progress in Nuclear Energy, 53: 207-211.

[7] Bashter I.I., Abdo A.E.S., Abdel-Azim M.S. 1997. Magnetite ores with steel or basalt for concrete radiation shielding. Japanese journal of applied physics, 36: 3692.

[8] Singh V.P., Badiger N.M. 2014. Gamma ray and neutron shielding properties of some alloy materials. Annals of Nuclear Energy, 64: 301-310.

[9] Singh V.P., Medhat M.E., Shirmardi S.P. 2015. Comparative studies on shielding properties of some steel alloys using Geant4, MCNP, WinXCOM and experimental results, Radiation Physics and Chemistry, 106: 255-260.

[10] Kaur S., Kaur A., Singh P.S., Singh T. 2016. Scope of Pb-Sn binary alloys as gamma rays shielding material. Progress in Nuclear Energy, 93: 277-286.

[11] Harish V., Nagaiah N., Prabhu T.N., Varughese K.T. 2009. Preparation and characterization of lead monoxide filled unsaturated polyester based polymer composites for gamma radiation shielding applications. Journal of applied polymer science, 112: 1503-1508.

[12] Mann K.S., Rani A., Heer M.S. 2015. Shielding behaviors of some polymer and plastic materials for gamma-rays. Radiation Physics and Chemistry, 106: 247-254.

[13] Kaewjaeng S., Kaewkhao J., Limsuwan P., Maghanemi U. 2012. Effect of BaO on optical, physical and radiation shielding properties of SiO2-B2O3-Al2O3-CaO-Na2O glasses system. Procedia Engineering, 32: 1080-1086.

[14] Ruengsri S. 2014. Radiation shielding properties comparison of Pb-based silicate, borate, and phosphate glass matrices. Science and Technology of Nuclear Installations, 5: 2014.

[15] Manonara S.R., Hanagodimath S.M., Gerward L., Mittal K.C. 2011. Exposure buildup factors for heavy metal oxide glass: a radiation shield. Journal of the Korean Physical Society, 59: 2039-2042.
[16] Ersundu A.E., Büyükyıldız M., Ersundu M.Ç., Şakar E., Kurudirek M. 2018. The heavy metal oxide glasses within the WO3-MoO3-TeO2 system to investigate the shielding properties of radiation applications. Progress in Nuclear Energy, 104: 280-287.
[17] Sayyed M.I., Lakshminarayana G., Kityk I.V., Mahdi M.A. 2017. Evaluation of shielding parameters for heavy metal fluoride based tellurite-rich glasses for gamma ray shielding applications. Radiation Physics and Chemistry, 139: 33-39.
[18] Sayyed M.I., Lakshminarayana G. 2018. Structural, thermal, optical features and shielding parameters investigations of optical glasses for gamma radiation shielding and defense applications. Journal of Non-Crystalline Solids, 487: 53-59.
[19] Singh K., Singh H., Sharma V., Nathuram R., Khanna A., Kumar R., Sahota H.S. 2002. Gamma-ray attenuation coefficients in bismuth borate glasses. Nuclear Instruments and Methods in Physics Research Section B: Beam Interactions with Materials and Atoms, 194: 1-6.
[20] Danilyuk P.S., Puga P.P., Krasilinets V.N., Gomonai A.I., Puga G.D., Rizak V.M., Turok I.I. 2018. X-ray Fluorescence of Eu 3+ Ions in Glassy and Polycrystalline Lithium Tetraborate. Glass Physics and Chemistry, 44 (1): 1-6.
[21] Kaplan M.F. 1989. *Concrete Radiation Shielding*. John Wiley and Sons Inc, 99s New York.
[22] Yorgun N.Y., Kavaz E., Oto B., Akdemir F. 2018. Evaluation of gamma-ray attenuation properties of lithium borate glasses doped with barite, limonite and serpentine. Radiochimica Acta, 106 (10): 865-872.
[23] Gerward L., Guilbert N., Jensen K.B., Leving H. 2004. WinXCom–a program for calculating X-ray attenuation coefficients. Radiation physics and chemistry, 71: 653-654.
[24] Büyükyıldız M. 2016. Effective atomic numbers and electron densities for some lanthanide oxide compounds using direct method in the energy region of 1 keV-20 MeV. Bitlis Eren Üniversitesi Fen Bilimleri Enstitüsü Dergisi, 6 (1): 7-12.
[25] Kavaz E. 2018. Investigation on Photon Interaction Properties of Some Polymers Used in Production of Hydrogels. Süleyman Demirel Üniversitesi Fen Edebiyat Fakültesi Fen Dergisi, 13 (2): 97-107.
[26] Bircan H., Manisa K., Atan A.S., Erdoğan M. 2017. Gama ve X-Işını Radyasyonu Yarı Değer Kalınlık Değerinin Hesaplanması için Yeni Bir Denklem. Süleyman Demirel Universitesi Fen Bilimleri Enstitüsü Dergisi, 12 (1): 23-29.
[27] Sayyed M.I., Kaky K.M., Gaikwad D.K., Agar O., Gawai U.P., Baki S.O. 2019. Physical, structural, optical and gamma radiation shielding properties of borate glasses containing heavy metals (Bi2O3/MoO3). Journal of Non-Crystalline Solids, 507: 30-37.
[28] Dikmen Z., Orhun Ö. 2013. Manyetik Modifiye Edilmiş Sentetik ve Doğal Zeolitlerin Hazırlanması Ve Bazı Fiziksel Özelliklerinin Kıyaslanması. Anadolu University of Sciences & Technology-A: Applied Sciences & Engineering, 14 (1): 75-90.
[29] Sayyed M.I., Akman F., Kaçal M.R., Kumar A. 2019. Radiation protective qualities of some selected lead and bismuth salts in the wide gamma energy region. Nuclear Engineering and Technology, 51: 860-866.
[30] Issa S.A., Sayyed M.I., Zaid M.H.M., Matori K.A. 2018. Photon parameters for gamma-rays sensing properties of some oxide of lanthanides. Results in Physics, 9: 206-210.
[31] Hine G.J. 1952. The effective atomic numbers of materials for various gamma ray processes. Physical Review, 85: 725.